ACS APPLIED MATERIALS & INTERFACES

RESEARCH ARTICLE

www.acsami.org

Chemically Cross-Linked Thin Poly(vinylidene fluoride-co-trifluoroethylene)Films for Nonvolatile Ferroelectric Polymer Memory

Yu Jin Shin,[†] Seok Ju Kang,[†] Hee Joon Jung,[†] Youn Jung Park,[†] Insung Bae,[†] Dong Hoon Choi,[‡] and Cheolmin Park[*,†]

[†]Department of Materials Science and Engineering, Yonsei University, Seoul, Korea

[‡]Department of Chemistry, Korea University, Seoul, Korea

ABSTRACT: Both chemically and electrically robust ferroelectric poly(vinylidene fluoride-co-trifluoro ethylene) (PVDF-TrFE) films were developed by spin-coating and subsequent thermal annealing with the thermal cross-linking agent 2,4,4-trimethyl-1,6-hexanediamine (THDA). Well-defined ferroelectric β crystalline domains were developed with THDA up to approximately 50 wt %, with respect to polymer concentration, resulting in characteristic ferroelectric hysteresis polarization-voltage loops in metal/cross-linked ferroelectric layer/metal capacitors with remnant polarization of approximately 4 μC/cm^2. Our chemically networked film allowed for facile stacking of a solution-processable organic semiconductor on top of the film, leading to a bottom-gate ferroelectric field effect transistor (FeFET). A low-voltage operating FeFET was realized with a networked PVDF-TrFE film, which had significantly reduced gate leakage current between the drain and gate electrodes. A solution-processed single crystalline tri-isopropylsilylethynyl pentacene FeFET with a chemically cross-linked PVDF-TrFE film showed reliable $I-V$ hysteresis with source-drain ON/OFF current bistablility of 1×10^3 at a sweeping gate voltage of $\pm$20 V. Furthermore, both thermal micro/nanoimprinting and transfer printing techniques were conveniently combined for micro/nanopatterning of chemically resistant cross-linked PVDF-TrFE films.

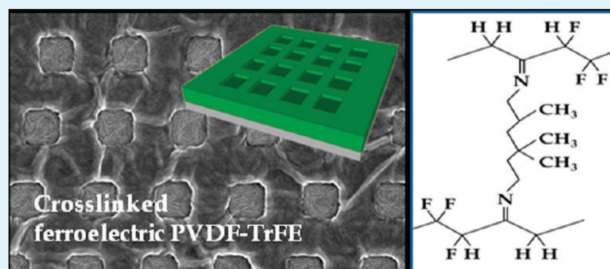

KEYWORDS: nonvolatile ferroelectric memory, 2,4,4-trimethyl-1,6-hexanediamine, PVDF-TrFE, capacitor, transistor memory, thermal cross-linking, micropatterning

1. INTRODUCTION

Next-generation memory is the focus of attention for new mobile, flexible, and ubiquitous computing applications, which will require a large storage capacity, as well as nonvolatile information storage.[1,2] Various types of nonvolatile memory are actively being investigated, one of which is based on ferroelectric polymers, that guarantee easy and cost-effective processing and mechanical flexibility of device.[3−6] Poly vinylidene fluoride (PVDF) and its TrFE copolymers (PVDF-TrFE) are representative ferroelectric polymers whose ferroelectricity originates from bistable dipole polarization between hydrogen and fluorine atoms, and have potential memory characteristics, such as good fatigue, long data retention, and large remnant polarization.[7−9] In addition to metal/ferroelectric/metal (MFM) capacitor-type destructive memory units in which a solution-processed ferroelectric layer is inserted between top and bottom electrodes, ferroelectric field effect transistors (FeFETs) have been introduced. Such FeFETs have a ferroelectric gate insulating layer, as well as an organic semiconducting layer due to nondestructive readout capability, electrical switching, mechanical flexibility, and small cell size.[10,11] The polarization state of the ferroelectric gate set by the polarity of the writing gate voltage controls the electrical conductance of the semiconductor channel and, thus, distinguishes the two logic states, which are the ON or OFF states of the channel current with respect to memory function.[1,12] Because spontaneous polarization directly controls channel conductance, neither ferroelectric cell capacitance nor the requirement for high polarization are determining factors in the device operation, which is potentially beneficial for high-density as well as low-power consumption.[13]

For a bottom-gate FeFET with a soluble organic semiconducting layer desirable for potential mass production, great care should be taken when choosing appropriate solvents that do not harm underlying ferroelectric polymer layer. In fact, direct spin-coating of a semiconductor solution on a PVDF-TrFE film frequently causes serious film damage, resulting in device failure. Indeed, only a few bottom gate FeFETs based on a solution process of organic and polymeric semiconductors have been successfully demonstrated,[1,10,14] whereas, in most cases, vacuum-deposited pentacene active channels were used.[14−16] In our previous studies, a single-crystalline tri-isopropylsilylethynyl pentacene (TIPS-PEN) active channel was solution-deposited by solvent exchange method on a spin-coated PVDF-TrFE layer. The resulting bottom gate FeFET showed highly reliable

Received: November 26, 2010
Accepted: January 17, 2011
Published: February 8, 2011

ACS Publications © 2011 American Chemical Society

nonvolatile memory performance with an ON/OFF ratio of approximately 1×10^3 at a gate voltage sweep of $\pm$30 V.[10]

Despite good memory performance, TIPS-PEN FeFET still requires a polymer interlayer, namely poly(vinyl phenol) (PVP), not only to prevent delamination of the ferroelectric film during formation of single crystals but also to reduce gate leakage current between drain and gate electrodes. This observation suggests that a PVDF-TrFE film should be both chemically and electrically resistant. To maximize the ON/OFF ratio at zero gate voltage, we should minimize molecular and structural defects arising from crystalline grain−grain mismatch and trapped residual solvent in entangled polymer chains in PVDF-TrFE films. A thick ferroelectric gate insulator may solve the leakage problem; however, as a consequence, it may also increase the operating gate voltage required for polarization switching of PVDF-TrFE with relatively large coercive electric field of approximately 50 MV/m. The selection of a proper solvent that can give rise to a thin and very dense PVDF-TrFE film is another way to reduce gate leakage. Viscous cylcohexanone has been successfully employed for top gate FeFET with PVDF-TrFE gate insulator.[17] Likewise, insertion of an additional interlayer between PVDF-TrFE and gate electrode has been proposed for controlling leakage.[18]Although various organic and inorganic interlayers have been incorporated for reducing gate leakage current, including SiO_2,[9,19] Ta_2O_5,[20] PVP,[21,22] poly(melamine-co-formaldehyde), and poly(styrene-random-methylmethacrylate) copolymer,[23] it would still be beneficial if one could use a single layered ferroelectric polymer film with both chemical and electrical resistance to allow for a facile solution stacking process, as well as low gate leakage current.

In this study, we present a facile route for fabricating both chemically and electrically robust ferroelectric PVDF-TrFE films applicable for nonvolatile memory units, such as MFMs and FeFETs. Our method is based on thermal cross-linking of a spin-coated PVDF-TrFE film by introducing the cross-linking agent 2,4,4-trimethyl-1,6-hexanediamine (THDA). The covalently networked ferroelectric film allows not only for facile stacking of a solution-processable organic semiconductor on top of the film, leading to a bottom-gate FeFET, but also for low-voltage operation by significantly reducing gate leakage current without the need for an additional interlayer. The solution-processed single crystalline TIPS-PEN FeFET with a cross-linked PVDF-TrFE film shows reliable $I-V$ hysteresis with ON/OFF current bistablility of 10^3 at a sweeping gate voltage of $\pm$20 V. We also demonstrate that both thermal micro/nanoimprinting and transfer printing techniques are conveniently combined to allow for various micro/nano patterning of cross-linked PVDF-TrFE films.

2. EXPERIMENTAL SECTION

Materials and Film Preparation. PVDF-TrFE with 25 wt % TrFE was purchased from MSI Sensors. All organic solvents, including methyl ethyl ketone (MEK), dimethylformamide (DMF), and cyclohexanone, were purchased from Sigma Aldrich Korea. The cross-linking agent,THDA, was kindly provided by Samsung Advanced Institute of Technology. The melting (T_m) and Curie (T_c) temperature of the PVDF-TrFE were 160 and 80 °C, respectively.

For cross-linked thin film fabrication, PVDF-TrFE/THDA blend solutions in MEK were spin-coated at 2000 rpm for 60 s on a highly boron-doped Si substrate by controlling the composition of the THDA from 0.2 to 100 wt % with respect to the weight of polymer. The spin-coated films were subsequently cured at 170 °C for 30 min for cross-linking, and then slowly cooled to room temperature.

Device Fabrication. For MFM capacitor fabrication, cross-linked PVDF-TrFE thin films were coated on a highly boron-doped Si substrate and Au top electrodes were vacuum-deposited on cross-linked films through a shadow mask with holes of 200 μm in diameter under pressure (1×10^6 mbar) and an evaporation rate of 0.1 nm/s. Furthermore, in order to fabricate the FeFET device, single-crystal TIPS-PEN was deposited on the cross-linked PVDF-TrFE film by the solvent exchange method as an active channel, as described in our previous study.[10] Square-shaped source and drain Au electrodes, the size and thickness of which were 200 μm and 100 nm, respectively, were thermally evaporated through a shadow mask on a single crystal of TIPS-PEN randomly deposited on the PVDF-TrFE surface. Preparation of a single crystal of TIPS-PEN, firmly bridged between source and drain electrodes, completed the fabrication of a bottom gate top contact FeFET memory.

Micropattern Fabrication. *1. Microimprinting.* A 250 nm thick PVDF-TrFE film was deposited on a highly doped Si and prepared by spin coating without further thermal curing. Subsequently, the prepatterned PDMS mold containing various square-shaped dents and mesas arrayed was placed on the PVDF-TrFE film with conformal contact, and then thermal-imprinting was performed at 170 °C for 30 min with a pressure of 1 kg using a custom apparatus. The squares are varied in size from 2 μm to 750 nm. The PDMS mold was fabricated by casting a PDMS precursor (Sylgard 184, Dow Corning Corp) on a photoresist master, as described elsewhere.[24]

2. Transfer Printing. To transfer the micropatterned PVDF-TrFE/THDA with Al layer, an Al layer with a thickness of 50 nm was deposited on the hexagonal-shaped PDMS stamp surface by thermal evaporation and subsequently a PVDF-TrFE/THDA film floated on the DI water was overlaid on the Al deposited PDMS mold. The transfer of the bilayer of (PVDF-TrFE/THDA)/Al selectively on the protrude regions of the PDMS mold was accomplished by putting the PDMS mold with the bilayer in conformal contact on a highly Boron doped Si substrate and thermally annealing at 170 °C for 30 min. Removing the stamp from the substrate completed the pattern transfer process.

Characterization. Morphologies of the cross-linked PVDF-TrFE films were analyzed with a scanning electron microscope (SEM, JEOL JSM-600F) and atomic force microscope in tapping mode (AFM, Digital Instruments NanoScope 3100). The crystalline structure of cross-linked PVDF-TrFE was characterized by two-dimensional (2D) Grazing-Incidence X-ray Diffraction (GIXD). GIXD was performed on the 4C2 beamline at the Pohang Accelerator Laboratory in Korea (incidence angle: 0.15°). Grazing incident reflection absorption spectra (GIRAS) were measured using a Bruker-IFS66 V spectrometer for analyzing the phase of the cross-linked PVDF-TrFE layer. Moreover, ferroelectric properties were determined using a virtual ground circuit (Radiant Technologies Precision LC units) and the electrical properties of the devices were recorded using semiconductor systems (E5270B, HP4284A, Agilent Technologies). All measurements were performed in a metallic shielded box at room temperature in air.

3. RESULTS AND DISCUSSION

Figure 1 shows the proposed mechanism of chemical cross-linking between PVDF-TrFE chains mediated by THDA. Among the many potential cross-linking techniques available for fluorinated polymers based on either reaction with chemical agents, such as diamines,[25,26] bisphenols,[27,28] and thiol−ene systems,[29] electron beam radiation,[30,31] or by introduction of an iodine or bromine monomer in the polymer chain,[26,32] we employed a representative diamine agent, THDA, because of its commercial availability and ease of modification for future applications.[26,33] Because of the good basicity of THDA due to

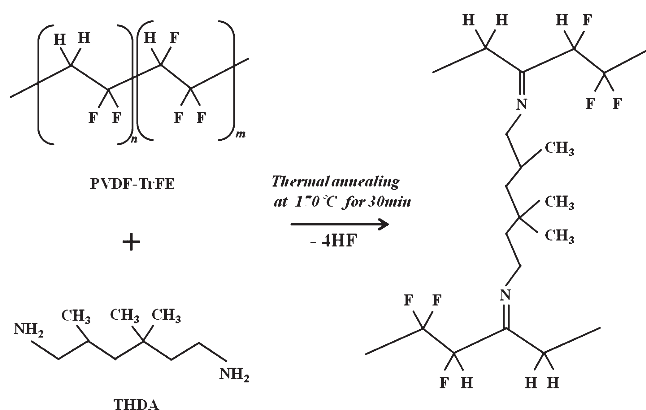

Figure 1. Schematic of the mechanism of cross-linking between PVDF-TrFE and THDA.

Table 1. Degree of Swelling of Cross-Linked PVDF-TrFE Films with Different Amounts of THDA in Various Solvents

THDA (wt%)	observation	τ_s (%) (solvent)
0	soluble	N/A
0.5	partially soluble	
1	insoluble	330 (MEK)
5	insoluble	254 (MEK)
10	insoluble	202 (MEK)
	insoluble	288 (DMF)
	insoluble	256 (THF)
	insoluble	210 (cyclohexanone)
	insoluble	19 (acetone)
20	insoluble	84 (MEK)

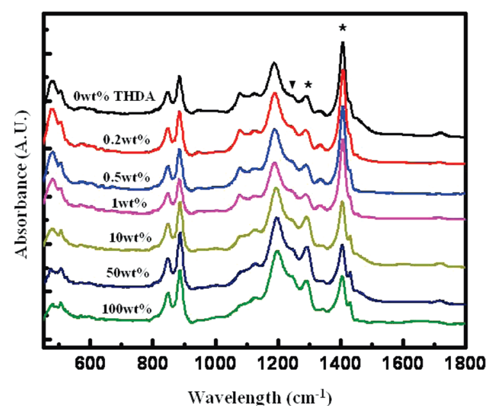

Figure 2. GIRAS spectra of cross-linked PVDF-TrFE films spin-coated onto an Al substrate with the addition of THDA from 0 to 50 wt % with respect to the amount of polymer. The characteristic absorbance peaks at 1289 and 1402 cm^{-1}, indicated with the asterisks, indicate the presence of β crystals and the orientation of polymer crystals with the chain axis perpendicular to the substrate. The absorbance at 1234 cm^{-1} indicated by a triangle corresponds to a characteristic peak for gamma crystals.

the electrodonating effect of its methyl and neopentyl groups, this diamine allows dehydrofluorination of a fluorinated polymer and forms a double bond between carbon and nitrogen atoms of fluorinated polymer, leading to chemical bridging between two fluorinated chains. Successful use of THDA for cross-linking has been demonstrated previously by Taguet et al., who cross-linked poly(VDF-co-HFP) chains, resulting in chemically and mechanically robust micrometer-thick films.[33]

Approximately 250 nm thick PVDF-TrFE films containing various amounts of THDA were readily spin-coated from homogeneous PVDF-TrFE/THDA blend solutions on Si substrates and subsequently annealed at 170 °C for 30 min for cross-linking. Uniform and transparent films were obtained after thermal treatment. To confirm the cross-linking of PVDF-TrFE with THDA, we performed a detailed investigation of dissolution and swelling of the cross-linked PVDF-TrFE films as a function of THDA in various solvents. For the dissolution test, we dipped cross-linked films with 10 wt % THDA for 2 h at 60 °C in 5 different common solvents namely, MEK, DMF, THF, acetone and cyclohexanone. Most PVDF-TrFE samples were insoluble; however, significant swelling of the films was observed, characterized by different interference colors depending on the solvent used as shown in Table 1. In addition, we evaluated the degree of cross-linking of a PVDF-TrFE film in MEK as a function of amount of THDA by the conventional swelling measurement in which the cross-linking degree (τ_s(%)) was calculated by a relation of $((W_S - W_I)/W_I)100$, where W_S and W_I are weights of a PVDF-TrFE film before and after swelling in a solvent, respectively. A significant swelling greater than 300% with 1 wt % THDA gradually decreases with THDA and the degree of swelling becomes approximately 80% with 20 wt % THDA. The results are summarized in Table 1.

Ferroelectric β crystals in the cross-linked PVDF-TrFE films were evaluated by GIRAS as a function of the amount of THDA, as shown in Figure 2. All IR spectra showed similar absorption bands, in particular, those characteristic of a ferroelectric β phase: one at 1289 cm^{-1} ($A_1, \vec{\mu} \| \vec{b}$) which corresponded to the trans-zigzag conformation for the VDF trans sequence and the other at 1402 cm^{-1} ($B_1, \vec{\mu} \| \vec{c}$) whose vibrational transition moment is parallel to the chain axis. We also examined the portion of β crystals with respect to γ ones from IR spectra by comparing the relative peak intensities of the spectra of 1289 and 1234 cm^{-1}. The absorbance at 1234 cm^{-1} corresponds to a characteristic peak for gamma crystals as indicated by a triangle in Figure 2. The fraction of β crystals calculated with a relation of $A_{1289}/(A_{1289} + A_{1234})$ is approximately 0.5 for all the samples, regardless of THDA, which implies that no significant transition occurred with THDA from β to γ crystals. Our results suggest that the ferroelectric β crystal phase is well-maintained, even after chain cross-linking.

It should be noted that the cross-linking of PVDF-TrFE with THDA was not clearly evidenced by IR spectroscope. Several references in the literature have dealt with the characterization of C═N bonds, i.e., imine groups by IR spectroscope. One shows that the imine group can be recognized with the characteristic absorbance at 1738 cm^{-1}, which is attributed to C═N stretching.[26] Another on the other hand, states that it is difficult to identify the C═N bond with explicit absorbance peaks and instead the imine group can be characterized with a broad absorption from 1650 to 1690 cm^{-1} by IR spectroscope.[34] In our system, exact identification of C═N was not readily made by IR spectroscope either although we have also observed a broad absorbance hump in the regions from 1650 to 1690 cm^{-1} in a cross-linked sample. The cross-linking of our samples with THDA was instead confirmed by systematic dissolution and swelling experiments previously described.

Surface crystalline molecular and micro structures of the cross-linked PVDF-TrFE films were further revealed by AFM and

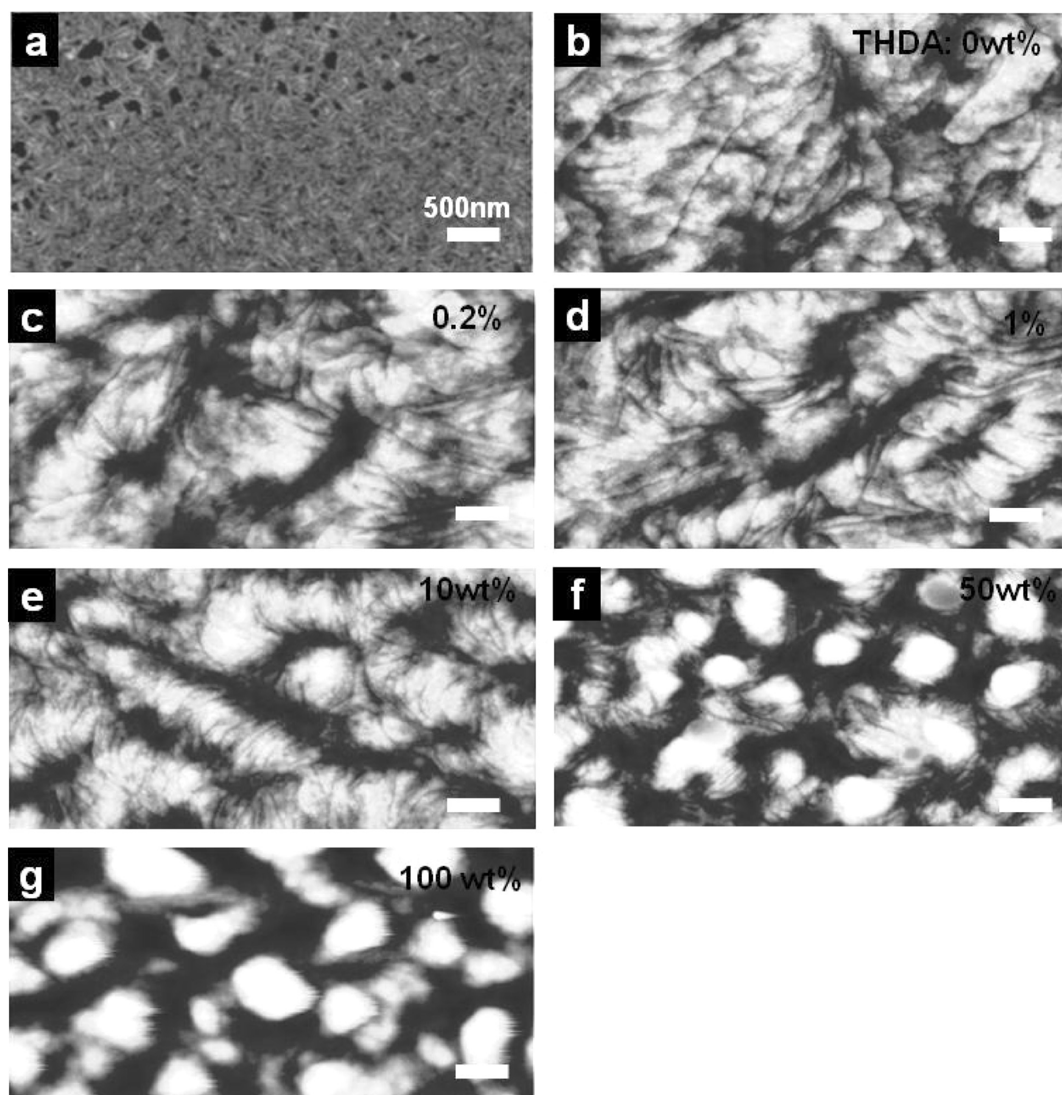

Figure 3. AFM images of the surface morphology of 250 nm thick PVDF-TrFE films: (a) thin film annealed at 135 °C for 2 h with edge-on crystals. Films melt-crystallized smooth surface after annealing at 170 °C for 30 min (b) without THDA, (c) 0.2 wt %, (d) 1 wt %, (e) 10 wt %, (f) 50 wt %, and (g) 100 wt % THDA. Rough surfaces in f and g resulted from the macrophase separation between PVDF-TrFE and THDA.

GIXD, as shown in Figures 3 and 4, respectively. Needlelike edge-on crystalline domains approximately 200 and 40 nm in length and width, respectively, were well-developed in the PVDF-TrFE film spin-coated and thermally annealed at 135 °C for 2 h without THDA, as shown in Figure 3a. The surface microstructure of a PVDF-TrFE film thermally annealed at 170 °C for 30 min was relatively smooth without a distinctive crystalline microstructure, as shown in Figure 3b. Our previous study demonstrated that the flat surface was attributed to the in-plane lamellar structure where the chain axis (*c*-axis) was dominantly normal to the substrate.[35] Thermal treatment of films with THDA for chemical cross-linking gave rise to a film surface similar to that of the film without the cross-linking agent. Interestingly, one can, however, notice that there exist a number of threadlike crystalline microdomains on the film surface when THDA is added as shown in Figure 3c−e. It is apparent that number of threadlike crystals increases with THDA. Further increase in THDA, however, resulted in bumpy surface aggregates because of macrophase separation in the samples as shown in Figure 3f and g.

Further study on the cross-linked PVDF-TrFE with THDA was performed with GIXD experiments, which allowed us to investigate the X-ray scattering from the cross-sectional planes of the cross-linked film. A PVDF-TrFE film spin-coated and thermally annealed at 135 °C for 2 h without THDA showed an intensified reflection on the meridian arising from the preferred (110) or (200) plane aligned along the film surface normal to the polymer chains on the surface.[35] It should be noted that because of the orthorhombic lattice of PVDF-TrFE crystals, which rather coincidently, are characterized by a $\sqrt{3}/2$ ratio of its *a* and *b* axes, nearly equal (200) and (110) spacings were observed. When the sample was heat-treated above T_m (~160 °C) different diffraction pattern was observed in which the preferred orientation of the {110}, {200} reflections were apparent near the equator, as shown in Figure 4b. These results indicate that the preferred alignment of the molecular chain axis *c* is perpendicular to the substrate surface, with both *a* and *b* axes parallel to the substrate. Samples thermally cured with THDA at 170 °C for 30 min also showed diffraction patterns similar to the one observed with a

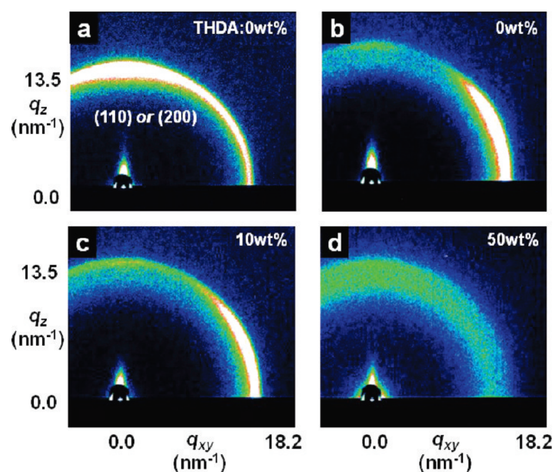

Figure 4. 2D GIXD patterns of PVDF-TrFE films (a) with intensified reflections on the meridian annealed at 135 °C for 2 h and the reflections on the equator, (b) annealed above T_m without THDA, and (c) cross-linked with 10 wt % THDA. (d) Diffused ring scattering was observed in films cross-linked with 50 wt % THDA because of the macrophase separation.

PVDF-TrFE film heat-treated above T_m, which implies that the threadlike crystalline texture observed with THDA in AFM does not affect the crystal orientation. For example, a cross-linked PVDF-TrFE film with 10 wt % THDA is shown in Figure 4c. When THDA was increased in blend films, the {110}, {200} reflections at the equator were diminished, disappearing completely at THDA content over 50 wt % with respect to PVDF-TrFE, as shown in Figure 4d. Considering that GIXD more clearly reveals surface structure of a thin film, the macro-phase separated bumpy domains observed at high THDA content in our AFM results in Figure 3 are attributed to amorphous PVDF-TrFE mixed with THDA evidenced by the diffused ring scattering in Figure 4d. GIXD did not, however, clearly visualize small PVDF-TrFE crystals, formed in between the bumpy amorphous domains, observed in GIRAS in Figure 2.

The ferroelectric polarization behavior of an approximately 250 nm thick PVDF-TrFE film was characterized using a typical polarization-applied voltage $(P-V)$ hysteresis loop with different concentrations of THDA, as shown in Figure 5a. A capacitor of the PVDF-TrFE film spin coated and subsequently annealed at 170 °C for 30 min on highly Boron doped Si electrode without THDA showed a typical hysteresis loop, resulting in a remnant polarization, P_r of approximately 4.51 $\mu C/cm^2$ and a coercive field, E_c of approximately 63.2 MV/m as shown in Figure 5a (black line). The P_r and E_c of a heat-treated sample above T_m were decreased and increased by approximately 30%, respectively, as compared with those of a PVDF-TrFE film annealed at 135 °C for 2 h. This result was due mainly to the preferred crystal orientation of the heat-treated film, with its *c*-axis perpendicular to the substrate during melting and recrystallization.[35] As cross-linked networks became denser by increasing the concentration of THDA, P_r and E_c values of cross-linked PVDF-TrFE film were very slightly decreased and increased, respectively, as shown in Figure 5a and Table 2. These results may arise mainly from the continuous decrease of the PVDF-TrFE fraction in homogeneously blended films with THDA. Different from the ferroelectric properties of cross-linked films with THDA from 0 to 10 wt %, a PVDF-TrFE film with a 50 wt % THDA blend ratio exhibited an abrupt decrease and increase of P_r and E_c, respectively, which may be ascribed to both phase-segregated, amorphous PVDF-TrFE and residual, nonreacted THDA.

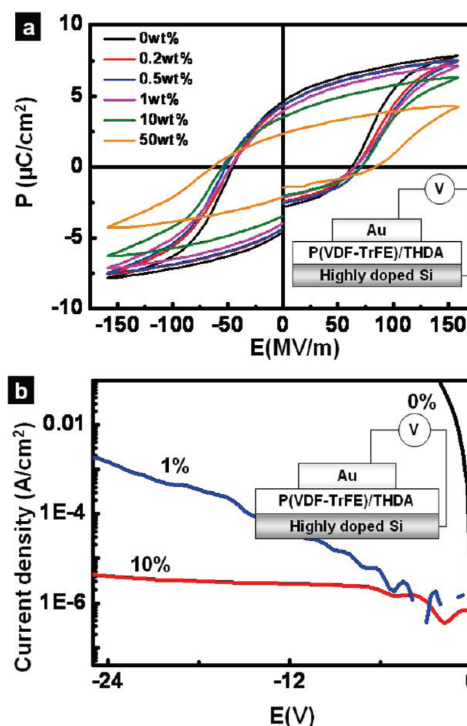

Figure 5. (a) Polarization *P* vs *E* hysteresis loops of metal/cross-linked PVDF-TrFE/metal capacitors with different ratios of THDA. (b) Leakage current density versus applied voltage behaviors of PVDF-TrFE films without and with THDA in MFM capacitors. A PVDF-TrFE film with 10 wt % THDA exhibits a significantly reduced current leakage as compared to one with 1 wt % THDA.The insets of a and b show schematics of the capacitors.

Table 2. Device Performance of MFM Capacitors with PVDF-TrFE Films with Various THDA Content[a]

PVDF-TrFE (thickness) (nm)	THDA (wt %)	P_r(μC/cm^2)	P_{max} (μC/cm^2)	E_c(MV/m)
250	0	4.51	7.53	63.2
	0.2	3.98	6.67	66.6
	0.5	3.94	6.57	67.8
	1	3.79	6.46	68.4
	10	3.42	6.18	70.2
	50	2.33	4.24	825
200	0	5.1	8.06	63.5
	0.2	4.42	7.61	63.3
	0.5	4.40	7.67	64.5
	10	4.34	7.58	76.5

[a] All ferroelectric properties are averaged out from 20 MFM cells.

The residual THDA of a sample with high THDA content may affect both ferroelectric and dielectric properties. Maximum amount of THDA which can be associated with PVDF-TrFE in our system is approximately 90 wt % of PVDF-TrFE when assumed that only VDF moiety can react with THDA as reported in the previous work.[33] As observed in Figure 3, when THDA was added to more than 50 wt % with respect to PVDF-TrFE in our experiments, the nonreacted, residual THDA seem to result in

Table 3. Device Performance of FeEETs with PVDF-TrFE Films with Various THDA Content

PVDF-TrFE/ THDA (thickness (nm)/wt%)	Memory Window(V)	I_{on} (A)	I_{off} (A)	$I_{on/off}$
250/0	N/A	N/A	N/A	N/A
250/0.2	9.75	2.68×10^{-8}	$1.18 \times 10^{-1}0$	$1 \times 10^{2.36}$
250/10	7.2	4.92×10^{-8}	9.90×10^{-12}	$1 \times 10^{3.67}$

micrometer level bumpy amorphous PVDF-TrFE domains phase-separated with ferroelectric, cross-linked PVDF-TrFE on the film surface. In the ferroelectric properties, as shown in Figure 5a, the amorphous domains gave rise to significant increase in the coercive field for ferroelectric switching. In the dielectric properties, the residual THDA with its dielectric constant of approximately 2.5 may lower the capacitance of a cross-linked PVDF-TrFE film with the dielectric constant of approximately 9. A similar tendency of ferroelectric capacitor properties with 250 nm thick PVDF-TrFE films varying THDA content was observed with 200 nm thick cross-linked PVDF-TrFE layers. The homogeneous and pinhole free films exhibited reduced coercive field and similar P_r values because of cross-linking as summarized in Table 3.

$I-V$ measurement of capacitors with various THDA amounts further suggested the role of THDA for reducing pin-holes and defects in the films, leading to a high breakdown voltage and low leakage current, as shown in Figure 5b. A 250 nm thick PVDF-TrFE film without THDA was electrically broken down, regardless of thermal annealing conditions, such as 170 °C for 30 min and 135 °C for 2 h. In contrast, cross-linked PVDF-TrFE films were able to withstand a bias voltage up to 25 V with significantly reduced current densities below 1×10^{-3} and 1×10^{-6} A/cm^2 for 1 and 10 wt % THDA, respectively. In particular, a film with 10 wt % THDA was very stable over a range of bias voltages, as shown in Figure 5b.

An electrically stable and topologically smooth film with THDA allowed us to realize a FeFET capable of operating at a low voltage with an organic semiconductor, TIPS-PEN. Our cross-linked film was also chemically robust enough to directly deposit ribbon-shaped single crystalline TIPS-PEN on its surface by solvent exchange method without the need for an additional interlayer, such as PVP. Thus, as shown in Figure 6a, we were able to fabricate a bottom gate-top contact FeFET after evaporation of Au source and drain electrodes. The single crystalline TIPS-PEN on a cross-linked PVDF-TrFE film was highly birefringent under cross-polarizers, as shown in the inset of Figure 6a, which provided a good charge carrier path between source and drain electrodes with the 200 nm thickness and 100 μm width, as shown in Figure 6a. Single crystal TIPS-PEN FeFETs with cross-linked films clearly exhibited the characteristic ferroelectric hysteresis curves of source-drain current (I_{DS}) as a function of gate voltage, as shown in Figure 6b. The sharp increase of I_{DS} with negative bias gate voltage arose from an excess hole accumulated in the single-crystal TIPS-PEN layer. Furthermore, when the gate voltage went back to zero, I_{DS} remained at the value saturated with the gate voltage of −20 V due to the nonvolatility of H−F dipoles in the ferroelectric PVDF-TrFE film. The subsequent positive gate voltage imposed on the device gradually switched the H−F dipoles with H atoms pointing to

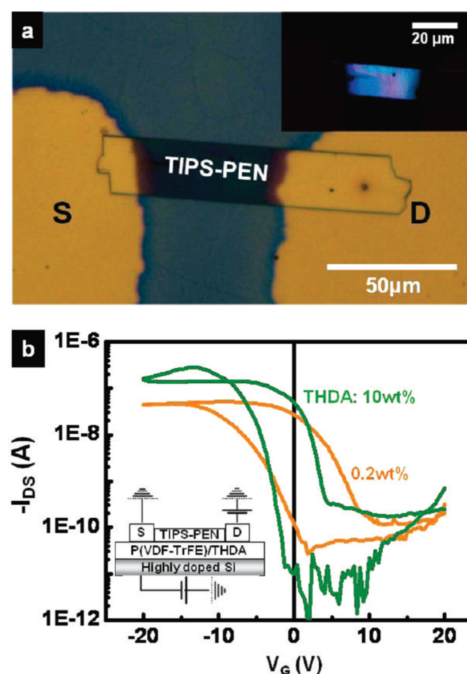

Figure 6. (a) OM image of single crystalline TIPS-PEN grown on 250 nm thick cross-linked PVDF-TrFE film. The inset shows the highly birefringent single crystalline TIPS-PEN under crossed polarizers. (b) Transfer characteristic curve ($I_{DS}-V_G$) of single-crystalline TIPS-PEN FeFETs containing cross-linked PVDF-TrFE films with 0.2 and 10 wt % THDA at a V_D of −5 V. A FeFET with 10 wt % THDA in cross-linked films exhibits an improved ON/OFF current ratio.The inset of b shows a schematic of the FeFET.

the TIPS-PEN layer, resulting in a rapid decrease in I_{DS}. Thus, the nonvolatility of polarization again made the current remaining the same, even after removal of positive voltage.

As expected from the results of $I-V$ measurement in Figure 5b, addition of THDA significantly reduced leakage current between gate and drain electrode, as well, giving rise to a low OFF current. For instance, a FeFET with a cross-linked PVDF-TrFE film containing 0.2 wt % THDA to the PVDF-TrFE displayed an ON and OFF current of approximately 2.68×10^{-8} and 1.18×10^{-10}A, respectively, leading to an ON/OFF ratio of approximately 100. On the other hand, a FeFET with 10 wt % THDA in a cross-linked PVDF-TrFE film exhibited much higher and lower ON and OFF currents of approximately 4.92×10^{-8} A and 9.90×10^{-12} A, respectively. In this case, the ON/OFF bistability ratio was approximately 5×10^3, which was more than 50 times greater than that of a device with 0.2 wt % THDA, as shown in Figure 6b. A device without THDA failed to show a characteristic hysteresis curve, due to severe gate leakage of the ferroelectric PVDF-TrFE layer. Detailed device performances of both cross-linked and uncross-linked PVDF-TrFE films are summarized in Table 3. A slightly higher ON current with the 10 wt % THDA sample may be simply attributed to the larger channel dimension (length x width) of single-crystalline TIPS-PEN whose size often depends on preparation conditions.

It is noteworthy that although the crystal orientation of PVDF-TrFE film with c-axis parallel to surface normal after thermally induced cross-linking is rather ineffective for maximizing ferroelectric polarization, the surface charge density of approximately 4 μC/cm^2 on the ferroelectric layer (Table 2) is still large enough to cause counter charges in organic semiconductor to accumulate

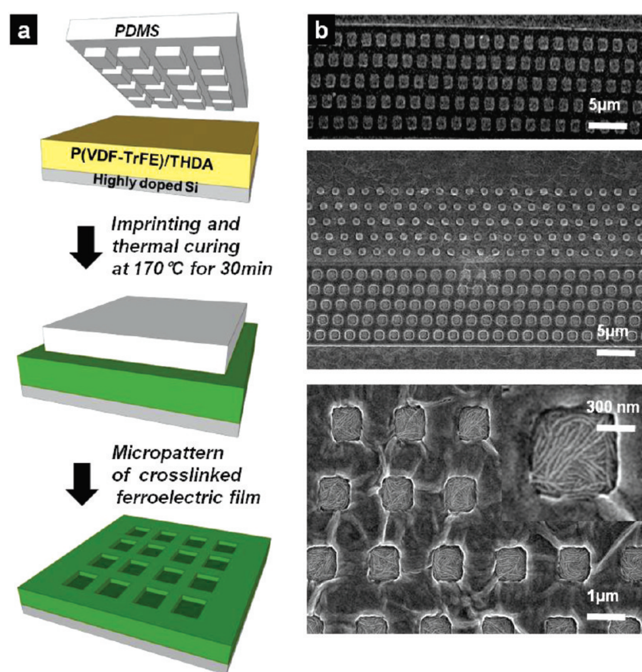

Figure 7. (a) Schematic procedure for the fabrication of cross-linked ferroelectric patterns by microimprinting. (b) SEM images of an imprinted ferroelectric film containing 10 wt % THDA obtained by applying a square PDMS pattern with dimensions from 2 μm to 750 nm. The magnified image of the imprinted 750 nm^2 PVDF-TrFE patterns in the inset shows the characteristic threadlike crystal domains arising from THDA.

at the channel and the ferroelectric layer interface, giving rise to a fully saturated source-drain current hysteresis curve. In fact, several previous works revealed that approximately 2 μC/cm^2 was required to saturate source-drain current in FeFET memories with organic semiconductors such as vacuum deposited poly[2-methoxy, 5-(2′-ethyl-hexyloxy)-*p*-phenylene-vinylene] (MEH-PPV),[1] pentacene,[15] and poly(3-hexylthiopene) (P3HT)[36] channels formed on PVDF-TrFE films. The field effect mobility values of single-crystal TIPS-PEN FeFETs with 10 wt % THDA samples were calculated from the slope of I_{DS} versus gate voltage (V_G) in Figure 6b, using an equation suitable for linear regime of drain current−voltage, because of the application of a low source-drain voltage (V_{DS}) of −5 V in our device. The equation is given by $I_{DS} = (W/2L)C_i\mu[2(V_G - V_T)V_{DS} - V^2_{DS}]$, where W and L are the width and length of the channel and C_i, μ, and V_T correspond to the capacitance per unit area of the PVDF-TrFE gate insulator, the field-effect mobility, and threshold voltage, respectively.[37] On the basis of this equation, the hole mobility values obtained were approximately 0.4 cm^2/(V s).

Furthermore, our thermally cross-linkable ferroelectric PVDF-TrFE films were readily combined with micro/nanoimprinting technology for generating facile micro/nanopatterns of cured PVDF-TrFE films. We employed a topographic PDMS mold with various dimensions of a square pattern and subsequently pressurized it on a PVDF-TrFE film containing 10 wt % THDA at 170 °C for 30 min, as schematically illustrated in Figure 7a. This process allowed us to fabricate various sizes of micropatterned PVDF-TrFE films up to submicrometer levels, which could then be thermally cured, thus making them chemically resistant to common organic solvents, as shown in Figure 7b. In particular, a square-shaped PVDF-TrFE pattern imprinted with a 750 nm edge length was produced. Interestingly, well-defined long crystalline domains were more densely developed in the pressurized squares, whereas rather featureless crystalline surface was shown outside. More detailed effect of pressure on cross-linking of a PVDF-TrFE film is under investigation.

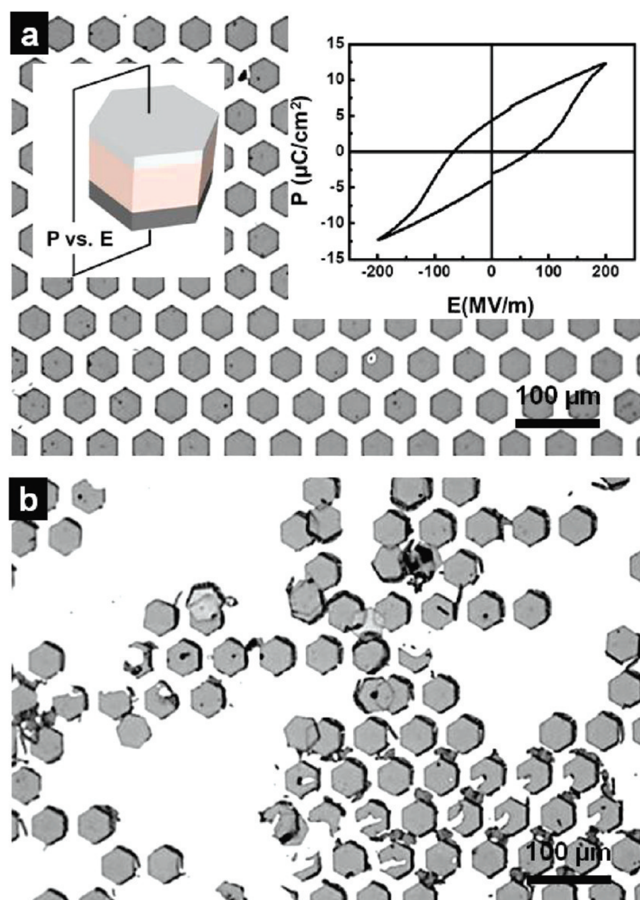

Figure 8. (a) OM image of the hexagonal arrays of Al/(PVDF-TrFE/THDA)/highly doped Si MFM microcapacitors fabricated by one step transfer printing. The inset of a on the left is a schematic of an isolated microcapacitor. The inset of a on the right is P vs E hysteresis loop from an isolated microcapacitor. (b) OM image of printed MFM microcapacitors without THDA after 30 min soaking in MEK at 60 °C.

A one-step transfer printing technique we have previously developed[11] was also employed to fabricate arrays of M/cross-linked PVDF-TrFE/M capacitors with high chemical resistance. Hexagonal-shaped MFM microcapacitors arrayed with *p6mm* symmetry was successfully fabricated as shown in Figure 8a. The polarization measurement of an isolated capacitor cell randomly selected from the patterned arrays shows a typical ferroelectric hysteresis loop with P_r and E_c of 4.4 μC/cm^2 and approximately 70 MV/m, respectively, as shown in the inset of Figure 8a. In an isolated small MFM cell, parasitic capacitances play a more stringent role with a large linear polarization, leading to higher P_s than values from Table 2.[11] Our printed MFM arrays with cross-linked PVDF-TrFE films turned out very resistant to organic solvents, in particular MEK, because arrays were not altered even after being soaked in MEK for 30 min at 60 °C. It is, however, apparent that printed MFM arrays without THDA were completely destroyed under the same conditions as shown in Figure 8b. Our strategy for micropatterning chemically cross-linked ferroelectric PVDF-TrFE films is apparently applicable

not only for nonvolatile memory applications but also for emerging transistor type sensors utilizing piezo and pyroelectric effect of chemically robust PVDF-TrFE.[38−41]

4. CONCLUSION

We employed a chemically and electrically robust thin ferroelectric PVDF-TrFE film for the fabrication of nonvolatile memory architectures, including MFM capacitors and FeFETs, by introducing a cross-linking method. Thin and cross-linked PVDF-TrFE films were prepared by spin-coating with the addition of the cross-linking agent (THDA) and subsequent thermal curing. Systematic investigation of thermally cured PVDF-TrFE thin films was performed such as chain conformation, film surface and crystal orientation. The chemically networked thin film had polarization hysteresis curves that were dependent on the voltage applied, which arose from the defined ferroelectric beta crystalline phase. Also, the cross-linked thin film on which a solution-processable organic semiconductor could be stacked was employed to fabricate a bottom gate FeFET. This thermally cured ferroelectric film had significantly reduced gate leakage without the need for any interlayer and, consequently, reliable $I-V$ hysteresis was obtained with a bistable ON/OFF ratio by applying a voltage of ±20 V. Furthermore, we demonstrated the patterning of cross-linked film by both thermal micro/nanoimprinting and transfer printing techniques, which can be applicable to the fabrication of device arrays.

■ AUTHOR INFORMATION

Corresponding Author

*Tel +82-2-2123-2833. Fax +82-2-312-5375. E-mail cmpark@yonsei.ac.kr.

■ ACKNOWLEDGMENT

This project was supported by The National Research Program for Memory Development sponsored by the Ministry of Knowledge and Economy, Republic of Korea. This work was partly supported by the IT R&D program of MKE/KEIT [100-30559, Development of next generation high-performance organic/nanomaterials and printing process technology] and the Seoul R&BD Program (10816). The X-ray experiments at PAL (4C2 beamline), Korea, were supported by MEST and POSCO, Korea. This work was supported by the Second Stage of the Brain Korea 21 Project in 2006 and National Research Foundation of Korea (NRF) grant, funded by the Ministry of Science and Technology (MEST), Republic of Korea (R11-2007-050-03001-0).

■ REFERENCES

(1) Naber, R. C. G.; Tanase, C.; Blom, P. W. M.; Gelinck, G. H.; Marsman, A. W.; Touwslager, F. J.; Setayesh, S.; de Leeuw, D. M. *Nat. Mater.* **2005**, *4*, 243.

(2) Sekitani, T.; Yokota, T.; Zschieschang, U.; Klauk, H.; Bauer, S.; Takeuchi, K.; Takamiya, M.; Sakurai, T.; Someya, T. *Science* **2009**, *326*, 516.

(3) Scott., J. C.; Bozano, L. D. *Adv. Mater.* **2007**, *19*, 1452.

(4) Naber, R. C. G.; Asadi, K.; Blom, P.W. M.; de Leeuw, D. M.; de Boer, B. *Adv. Mater.* **2010**, *22*, 933.

(5) Furukawa, T.; Takahashi, Y.; Nakajima, T. *Curr. Appl. Phys.* **2010**, *10*, e62.

(6) Park, Y. J.; Bae, I.; Kang, S. J.; Chang, J.; Park, C. *IEEE Trans. Dielectr. Electr. Insul.* **2010**, *17*, 1135.

(7) Lovinger, A. J. *Science* **1983**, *220*, 1115.

(8) Asadi, K.; de Leeuw, D. M.; de Boer, B.; Blom, P. W. M. *Nat. Mater.* **2008**, *7*, 547.

(9) Park, Y. J.; Chang, J.; Kang, S. J.; Park, C. *Appl. Phys. Lett.* **2009**, *95*, 102902.

(10) Kang, S. J.; Bae, I.; Park, Y,J.; Park, T. H.; Sung, J.; Yoon, S. C.; Kim, K. H.; Choi, D. H.; Park, C. *Adv. Funct. Mater.* **2009**, *19*, 1609.

(11) Kang, S. J.; Park, Y. J.; Bae, I.; Kim, K. J.; Kim, H. C.; Bauer, S.; Thomas, E. L.; Park, C *Adv. Funct. Mater.* **2009**, *19*, 1.

(12) Nguyen, C. A.; Lee, P. S.; Mhaisalkar, S. G. *Org. Electron.* **2007**, *8*, 415.

(13) Yoon, S. M.; Yang, S.; Byun, C.; Park, S. H.; Cho, D. H.; JungS., W.; Kwon, O. S.; Hwang., C. S. *Adv. Funct. Mater.* **2010**, *20*, 921.

(14) Choi, C. W; Prabu, A. A.; Kim, Y. M.; Yoon, S.; Kim, K. J.; Park, C. *Appl. Phys. Lett.* **2008**, *93*, 182902.

(15) Nguyen, C. A.; Mhaisalkar, S. G.; Lee, P. S. *Org. Electron.* **2008**, *9*, 1087.

(16) Unni, K. N. N.; de Bettignies, R.; Dabos-Seignon, S.; Nunzi, J. *Appl. Phys. Lett.* **2004**, *85*, 1823.

(17) Naber, R. C. G.; de Boer, B.; Blom, P. W. M.; de Leeuw, D. M. *Appl. Phys. Lett.* **2005**, *87*, 203509.

(18) Miller, S. L.; McWhorter, P. J. *J. Appl. Phys.* **1992**, *72*, 5999.

(19) Salvatore, G. A.; Bouvet, D.; Stolitchnov, I.; Setter, N.; Ionescu, A. M. *38th European Solid-State Device Research Conference, ESSDERC 2008*; Edinburgh, Scotland, U.K., Sept 15−19, 2008 ; IEEE: Piscataway, NJ, 2008; p 162.

(20) Fujisaki, S.; Ishiwara, H.; Fujisaki, Y *Appl. Phys. Lett.* **2007**, *90*, 162902.

(21) Kang, S. J.; Park, Y. J.; Sung, J.; Jo, P. S.; Park, C.; Kim, K. J.; Cho, B. O. *Appl. Phys. Lett.* **2008**, *92*, 012921.

(22) Noh, S. H.; Choi, W.; Oh, M. S.; Hwang, D. K.; Lee, K.; Im, S.; Jang, S.; Kim, E. *Appl. Phys. Lett.* **2007**, *90*, 253504.

(23) Chang, J.; Shin, C. H.; Park, Y. J.; Kang, S. J.; Jeong, H. J.; Kim, K. J.; Hawker, C. J.; Russell, T. P.; Ryu, D. Y.; Park, C. *Org. Electron.* **2009**, *10*, 849.

(24) Kim, H.; Yoon, B.; Sung, J.; Choi, D. G.; Park, C. *J. Mater. Chem.* **2008**, *18*, 3489.

(25) Schmiegel, W. W.; Logothetis, A. L. *ACS Symp.* **1984**, 159.

(26) Taguet, A.; Ameduri, B.; Boutevin, B. *Adv. Polym. Sci.* **2005**, *184*, 127.

(27) Schmiegel, W. W. *Angew. Makromol. Chem.* **1979**, *76*, 39.

(28) Pianca, M; Bonardelli, P; Tato, M; Cirillo, G; Moggi, G. *Polymer* **1987**, *28*, 224.

(29) Ameduri, B.; Boutevin, B.; Kostov, G. K.; Petrova, P. *Des. Monomers Polym.* **1999**, *2*, 267.

(30) Banik, I.; Bhowmick, A. K. *J. Mater. Sci* **2000**, *35*, 3579.

(31) Soresi, B.; Quartarone, E.; Mustarelli, P.; Magistris, A.; Chiodelli, G. *Solid State Ionics* **2004**, *166*, 383.

(32) Finlay, J. B.; Hallenbeck, A.; MacLachlan, J. D. *J. Elast. Plast.* **1978**, *10*, 3.

(33) Taguet, A.; Ameduri, B.; Dufresne, A. *Eur. Polym. J.* **2006**, *42*, 2549.

(34) Socrates, G. *Infrared and Raman Characteristic Group Frequencies: Tables and Charts*, 3rd ed.; John Wiley & Sons: Chichester, U.K., 2001.

(35) Park, Y. J.; Kang, S. J.; Park, C.; Kim, K. J.; Lee, H. S.; Lee, M. S.; Chung, U.; Park, I. J. *Appl. Phys. Lett.* **2006**, *88*, 242908.

(36) Naber, R. C. G.; Mulder, M.; De Boer, B.; Blom, P. W. M.; De Leeuw, D. M. *Org. Electron.* **2006**, *7*, 132.

(37) Fadlallah, M.; Benzarti, W.; Billiot, G.; Eccleston, W.; Barclay, D. *J. Appl. Phys.* **2006**, *99*, 104504.

(38) Oiu, X. *J. Appl. Phys.* **2010**, *108*, 011101.

(39) Graz, I.; Kaltenbrunner, M.; Keplinger, C.; Schwodiauer, R.; Bauer, S.; Lacour, S. P.; Wagner, S. *Appl. Phys. Lett.* **2006**, *89*, 073501.

(40) Zirkl, M.; Haase, A.; Fian, A.; Schon, H.; Sommer, C.; Jakopic, G.; Leising, G.; Stadlober, B.; Graz, I.; Gaar, N.; Schwodiauer, R.; Bauer-Gogonea, S.; Bauer, S. *Adv. Mater.* **2007**, *19*, 2241.

(41) Graz, I.; Krause, M.; Bauer-Gogonea, S.; Bauer, S.; Lacour, S. P.; Ploss, B.; Zirkl, M.; Stadlober, B.; Wagner, S. *J. Appl. Phys.* **2009**, *106*, 034503.